Anal. Bioanal. Electrochem., Vol. 16, No. 2, 2024, 205-216
https://www.doi.org/10.22034/abec.2024.711556

Analytical & Bioanalytical Electrochemistry

Full Paper

Electrochemical Study and Characterization: Exploration and Analysis of Electrodeposition of Hydroxyapatite on 316L Stainless Steel in A Physiological Environment

Nassima Bou-ydia, Hajar Atmani,* Mustapha Boulghallat, Ahmed Jouaiti, and Latifa Laallam

Laboratory of Molecular Chemistry, Materials and Catalysis, Sustainable Development Team, Sultan Moulay Slimane University, Beni Mellal, Morocco

*Corresponding Author, Tel.: +12632343883
E-Mail: atmani.hajar@usms.ma

Received: 25 December 2023 / Received in revised form: 10 February 2024 / Accepted: 20 February 2024 / Published online: 29 February 2024

Abstract- In this study, Hydroxyapatite coatings were electrochemically deposited into 316L stainless steel to be used in biomedical applications, such as bone implants. In this regard, the current investigation was conducted on a physiologically mimicked environment to emphasize its effects on the durability and biocompatibility of the coated stainless steel. The study accentuates on three kinds of stainless-steel surfaces: Blank 316L stainless steel surface (SS-316L), Anodized surface (ANSS-316L), and Hydroxyapatite treated surface (HASS-316L). The coating surface has been done by a solution containing 0.042 mol/L of calcium nitrate tetrahydrate (Ca (NO3)24H2O) and 0.025 mol/L of orthophosphoric acid. To examine the electrochemical behavior of the three samples and determine their characteristics, Fourier-transform infrared spectroscopy (FTIR), scanning electron microscopy (SEM), X-ray diffraction (XRD), and polarization Tafel curves with electrochemical impedance spectroscopy (EIS), have been used. The outcomes demonstrate that hydroxyapatite deposited on stainless steel increases the corrosion resistance of metal implants which may enhance its durability and biocompatibility.

Keywords- Hydroxyapatite; Electrodeposition; Orthopedic; Stainless steel; Metal implants

1. INTRODUCTION

Numerous investigations on orthopedic implants, especially metal implants, have been undertaken during the last several decades[1-3]. Unfortunately, their disintegration and corrosion in human bodies encouraged a number of scientists to look for an alternative [4]. The products of this corrosion trigger inflammatory responses causing tumors and undesirable diseases inside the human body [5]. Biological and mechanical qualities, such as biocompatibility and corrosion resistance, make stainless steel (316L) a potential material for use in biological implants. Its cheap price, commercial viability, ability to resist corrosion, and high mechanical qualities distinguish it. However, some medical research indicates that during corrosion of stainless steel used as orthopedic biomaterials in a physiologically relevant environment, complex species are produced and have a significant impact on the passivation behavior of the latter [6,7]. To overcome this problem, coating is considered the most useful solution [8-10]. Due to its biocompatibility, bioactivity, and similar chemical composition to bone tissue, hydroxyapatite (HAP) : $Ca_{10}(PO_4)_6(OH)_2$ can be used as coating product to enhance the medical activity of metallic organ implants [11]. As a result of this process, metal implants can integrate more effectively with the bone, since the metals can be provided with properties to promote protein adsorption and cell adhesion.

Several methods were used to apply HAP coatings to metal implants. Some of these methods include plasma spraying [12], immersion coating [13], electrophoresis deposition [11], and sol-gel deposition [5]. Electrochemical deposition [10] is the most widely used method, the principle of this technique is based on immersing the substrates in a hydroxyapatite solution (0.042 mol/L of calcium nitrate tetrahydrate ($Ca(NO_3)_2 4H_2O$) and 0.025 mol/L of orthophosphoric acid, Ca/P molar ratios of 1.67 in pH= 4.4) and applying an electric voltage to them (a direct current of type WYJ-3A for 2h in a two-electrode cell, considering platinum as the counter electrode, and 316L stainless steel as the anode). The substrates can be coated with hydroxyapatite electrochemically in one step. Commonly, challenges related to non-adhesive surface coatings arise, but anodizing stands out as a significant technique employed to mitigate such issues. Additionally, anodizing serves as a surface treatment that enhances paint adhesion and shields stainless steel from anodic oxidation (A solution of H_2SO_4 and HNO_3 (1:1)) [14].

The objective of this research is to explore the one-step electrodeposition process of hydroxyapatite (HAP) into stainless steel by using a protocol based on calcium and phosphorus ions to facilitate the formation of HAP. However, to improve the stability and the feasibility of the hydroxyapatite coating, the research examines also the impact of the anodization on the surface behavior of 316L stainless steel during the formation of a one-step electrochemical hydroxyapatite coating. This is achieved by scanning the surface morphology and stabilizing the electrochemical properties of 316L stainless steel.

This study aims to explore the synergy between stainless steel coated with hydroxyapatite (HAP) in a physiological mimic environment. The objective is to confirm the sustainability, biocompatibility of orthopedic implants and to determine the effect of hydroxyapatite on the corrosion of metallic implants and to confirm the results found in the literature. The investigation also includes an assessment and comparison of the surface characteristics and corrosion behavior of three types of stainless steel:

- Blank 316L stainless steel (SS-316L)
- Anodized surface (ANSS-316L)
- Hydroxyapatite-treated surface (HASS-316L)

2. MATERIALS AND METHODS

2.1. Stainless steel preparation (SS-316L)

Circles of medical-grade stainless steel (316L) were cut using laser technology to a diameter of 1.5 cm, then manually polished (with abrasive paper), washed with distilled water and acetone to eliminate surface contaminants, and drying them in the air.

Table 1. Chemical composition of stainless steel 316L

Elements	**Cr**	**Si**	**Mn**	**P**	**C**	**Ni**	**Mo**	**Cu**	**S**	**Fe**
%	16.35	0.50	1.30	0.030	0 .03	9.69	1.92	0.37	0.008	68.867

2.2. Anodization (ANSS-316L)

The anodization treatment before deposition is a primordial process that facilitates the hydroxyapatite coating on the metal implants. A solution of H_2SO_4 and HNO_3 (1:1) [14] was used as electrolyte for the anodic oxidation. Then, at room air (25°C) the anodizing was conducted by applying a voltage of 3.5 V for 15 min (which, as our experiments have shown, provides superior anodization than the 5-minute treatment) using two-electrode cell, platinum as the counter electrode and 316L stainless steel as the anode one. After anodic oxidation, 316L stainless steel is rinsed with distilled water and subsequently air dried.

2.3. Electrochemical deposition of hydroxyapatite (HASS-316L)

The protocol developed for the deposition of hydroxyapatite is based on the work of ZHANG Yuan-yuan [15], By applying a direct current of type WYJ-3A for 2h in a two-electrode cell, considering platinum as the counter electrode, and 316L stainless steel as the anode, a solution was prepared by dissolving 0.042 mol/L of calcium nitrate tetrahydrate

($Ca(NO_3)_2.4H_2O$) and 0.025 mol/L of orthophosphoric acid in distilled water to obtain suspensions with Ca/P molar ratios of 1.67 and the pH of solution was corrected to 4.4 by HNO_3 and NH_4OH.

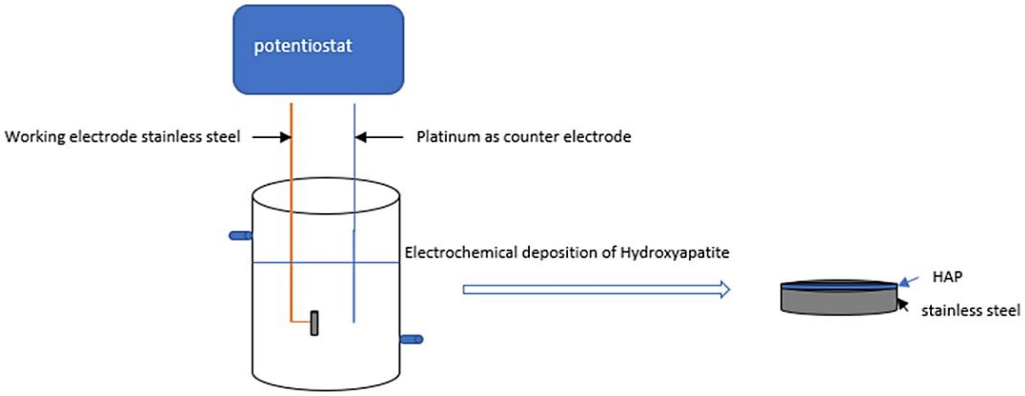

Figure 1. Schematic electrochemical deposition of HAP on the 316L stainless steel, the HAP coating on the substrate surface is formed by electrochemically generated OH^- ions and HPO_4^{2-} ions reacting with the Ca^{2+} ions present in the electrolyte solution

2.4. Characterization techniques

Prior to the electrochemical investigation, coated stainless steel was heated to 350 °C for an hour to improve findings and guarantee a strong HAP binding [16].

2.4.1. X-ray diffraction

After coating the stainless steel with hydroxyapatite, the crystalline phases in this compound are detected and their crystallographic forms are determined by the x-ray diffraction method. The HAP coating on 316L stainless steel was characterized using a Bruker D8 Advance type diffractometer and Cu-K radiation over a 2θ range from 15◦ to 65◦ at room temperature.

2.4.2. Fourier-transform infrared spectroscopy (FTIR)

A sample of HAP powder was scratched-off of coated stainless steel after electrochemical deposition, and its FTIR spectrum is shown in Figure.3 the JASCO FTIR spectrophotometer was used to record the spectrogram, which was taken between 4000 and 500 cm^{-1}.

2.4.3. Electrochemical study

The electrochemical study was carried out in a 0.9% NaCl solution using a three-electrode cell connected to a potentiostat. The experimental setup includes a potentiostat type Origaflex and a saturated calomel electrode (SCE) serving as the reference electrode, a platinum disc acting as the counter electrode, and a working electrode composed of 316L stainless steel.

The free potential measurement for 30min was accomplished using the electrochemical method "Polarization for corrosion (Tafel)" in a potential range of -1000 to 2000 mv with a stability time of 20 seconds and a scanning speed of 1mv per second. Moreover, an electrochemical impedance spectroscopy (EIS) was carried out at free potential in the corrosive medium in a linear regime with a sinusoidal signal of amplitude 20mv and ranging frequency from 10 kHz to 0.1 Hz.

3. RESULTS AND DISCUSSION

3.1. X-ray diffraction

Diffraction peaks are visualized in the XRD patterns (Figure 2) and we observed that at two Theta the HAP are represented by the values 28.80, 32.38 ,36.84 and 51.09. These results are satisfactory with the X-ray diffraction found in the literature [18] and it is confirmed by the results of the phase analysis of the diffraction data carried out using MATCH software, which compares the diffraction pattern of our sample with a database containing reference patterns in order to identify the phases present. The results of the diffractogram shown in the (Figure 2) indicate that HAP was well crystallized according to our protocol.

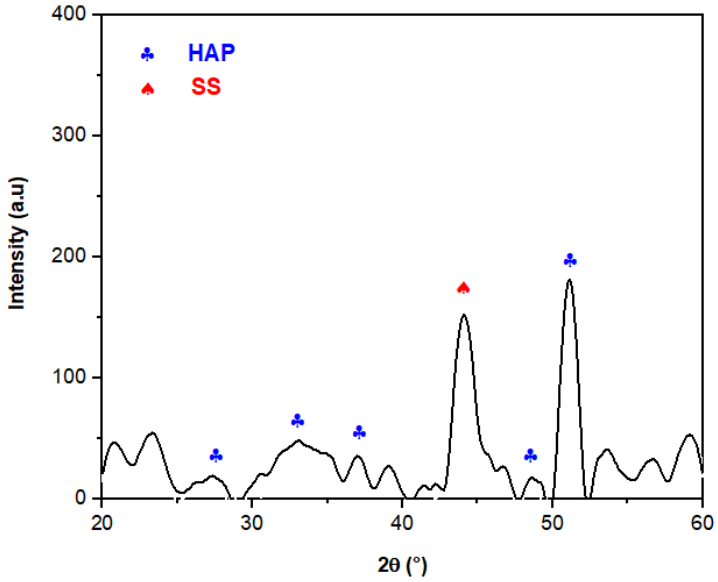

Figure 2. XRD pattern of HAP coating stainless steel (HASS-316L)

3.2. Fourier-transform infrared spectroscopy (FTIR)

The FTIR spectrum of synthesized HAP Figure 3 reveals the presence of CO_3^{2-} functional group in HAP could be identified by characteristic bands that appear at 878 cm^{-1} (characteristic to the ν_2 vibration mode), 1420 cm^{-1} (attributed to ν_1 symmetric $CO^{2-}{}_3$) and at 1750 cm^{-1} (ν_1+ ν_4 asymmetric) [19]. Peaks for the O-P-O bond stretch can be seen at 599 cm^{-1} and 564 cm^{-1}, for the P-O bond stretch at 1016 cm^{-1}, and for the O-H bond stretch at 2923 cm^{-1} [11].

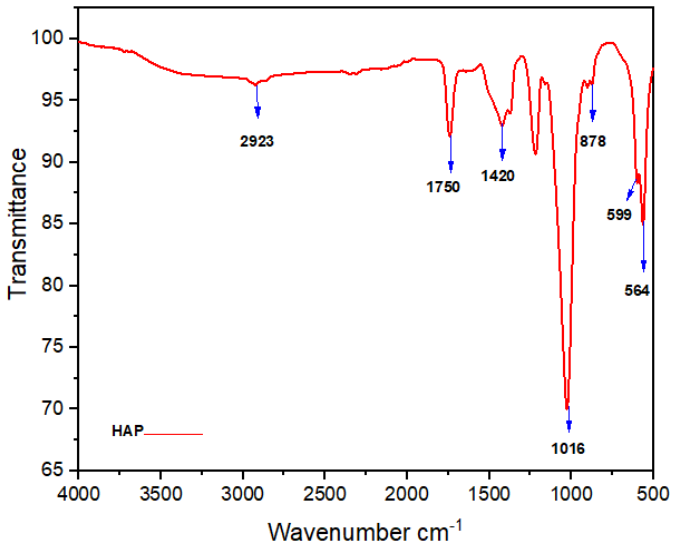

Figure 3. FTIR spectrum of hydroxyapatite powder

3.3. Scanning electron microscopy (SEM)

SEM pictures of the SS-316L, ANSS-316L and HASS-316L are shown in Figure.4, picture 4A appears the surface of the untreated stainless steel 316L while picture 4B shows the surface of the stainless steel 316L after an anodizing treatment. It can be seen that the surface is cracked, which lets the large-scale holes formed.

Electrochemical deposition led to the formation of a layer of solid HA phase, as seen in SEM pictures 4C with low and high magnification. It is remarkable that the form of primary needle-like crystals developed from the center of the holes and oriented in a flower-like shape after increasing the anodization time to 15 minutes, which facilitates the formation of the layered of HAP particles by a germination that starts from the holes and forms a coating deposited on the substrate of stainless steel 316L.

3.4. Polarization curves in the corrosive medium

Figure 5 shows the polarization potential curves (a) and Tafel diagrams (b) for the three surfaces. The findings demonstrate how anodizing and depositing alter the electrochemical properties of the investigated surfaces. The curves indicate the influence of HAP treatment on the behavior of the surfaces (a), and we noted that the corrosion potential value is retreated from the curves for surfaces without HAP Figure .5 (b): (SS-316L; ANSS-316L) towards those treated surface with HAP Figure.5 (b): (HASS-316L).

The hydroxyapatite layer provides a protection to the treated surfaces which explains the slowly. Corrosion potential (Ecorr), current corrosion density (Icorr), anodic and cathodic slopes, and polarization resistance (Rp) are all listed in Table .2 with; SS-316L, ANSS-316L and HASS-316L.

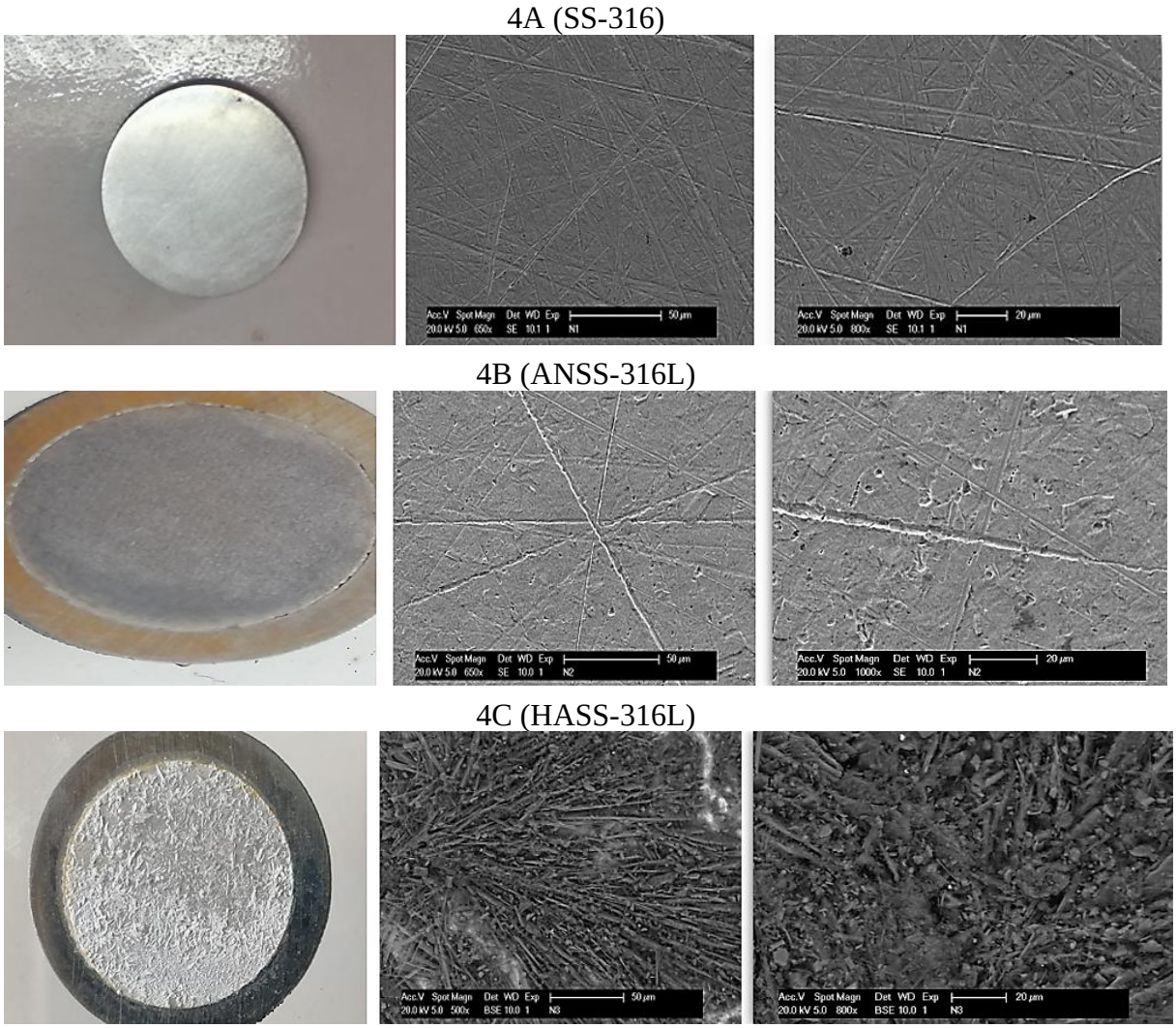

Figure 1. Samples and SEM Morphologies of SS-316L, ANSS-316L and HASS-316L at 50 µm and 20 µm

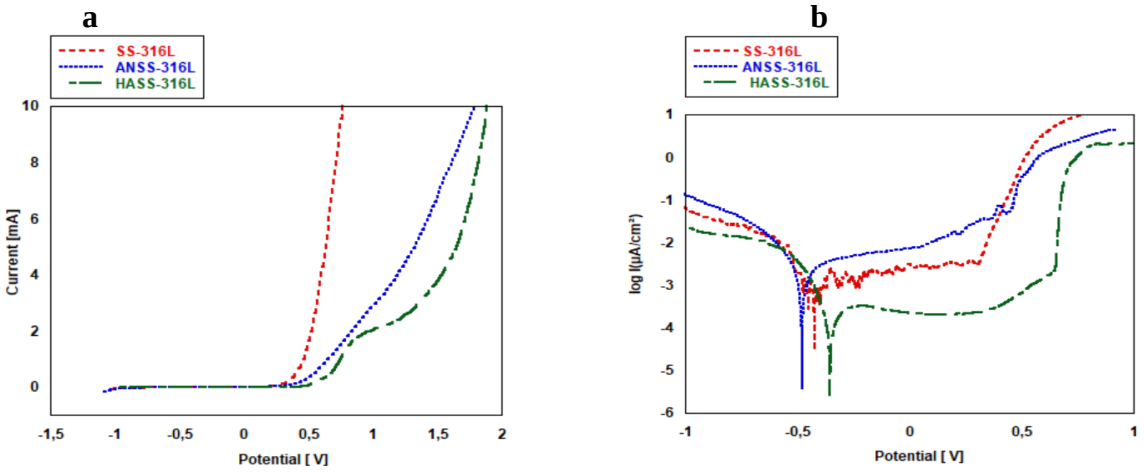

Figure 5. Polarization curves and Tafel diagrams of the stainless steel 316L with and without treatment

Table 2. Electrochemical results of tree surface according to Saturated calomel electrode (SCE)

Surface	**E_{corr} (mV)**	**I_{corr} (µA/cm²)**	**R_p (kohm.cm²)**	**β_C (mV)**	**β_a (mV)**	**Corrosion rate (µm/Year)**
SS-316L	-430.155	4.6	3.72	348.7	-363.2	54.336
ANSS-316L	-478.5	4.4	19.10	2512.3	-349.1	51.015
HASS-316L	-353.8	0.1200	164.71	217.1	-77.4	1.4035

Electrochemical studies (Table 2) reveal that HAP electrochemical deposition significantly improves stainless steel's resistance to corrosion. Compared to SS-316L and ANSS-316L, the polarization resistance of HASS-316L is substantially greater compared to ANSS-316L and SS-316L respectively (164.71>19.10>3.72 (kohm.cm²), and its corrosion rate is lower than ANSS-316L and SS-316L (54.336>51.015>1.4035 (µm/Year).

3.5. Electrochemical impedance spectroscopy (EIS)

To characterize the corrosion mechanism of SS-316L, ANSS-316L and HASS-316L electrochemical impedance measurement are carried out from 10 KHz to 0.1 Hz with a disturbance amplitude of 20 mV. Electrochemical impedance is a multifaceted concept that includes solution resistance, interface capacitance, charge transfer resistance, and mass transfer resistance. Their behavior varies depending on the frequency: at high frequency, the resistance of the solution is dominant, while at low frequency, charge transfer and mass transfer play a major role in the impedance.

To analyze this complex phenomenon, analysts typically use Nyquist diagrams, which represent the imaginary part of the impedance versus the real part [17].

The results of this method are obtained in the form of Nyquist diagram; Figure 6 and Figure 7 analysis of the Impedance spectrum makes it possible to associate representative physical parameters for each observable step on the diagram.

This can be approached by modeling spectrum by proposing equivalent electrical circuit (EEC). Figure 6 exposes the experimental impedance spectra carried out and the electrical circuits (EEC) corresponding to each spectrum it also illustrates the resistances R and capacitances C of the various surfaces. furthermore, the influence of the treatments on the form of the impedance spectra and the values of the resistances and capacities of the equivalent circuits can be observed in these data. The slopes of the ANSS316L m=0.89 (c) and HASS316L m=1.43 (e) spectra are much greater than that of the SS316L m=0.52 (a) spectrum, and it is also noted that the coated stainless-steel surface represents a high corrosion resistance and a high capacitance compared to the other surfaces which prove that the hydroxyapatite layer on

the stainless steel provides excellent protection against corrosion in the physiological mimic environment.

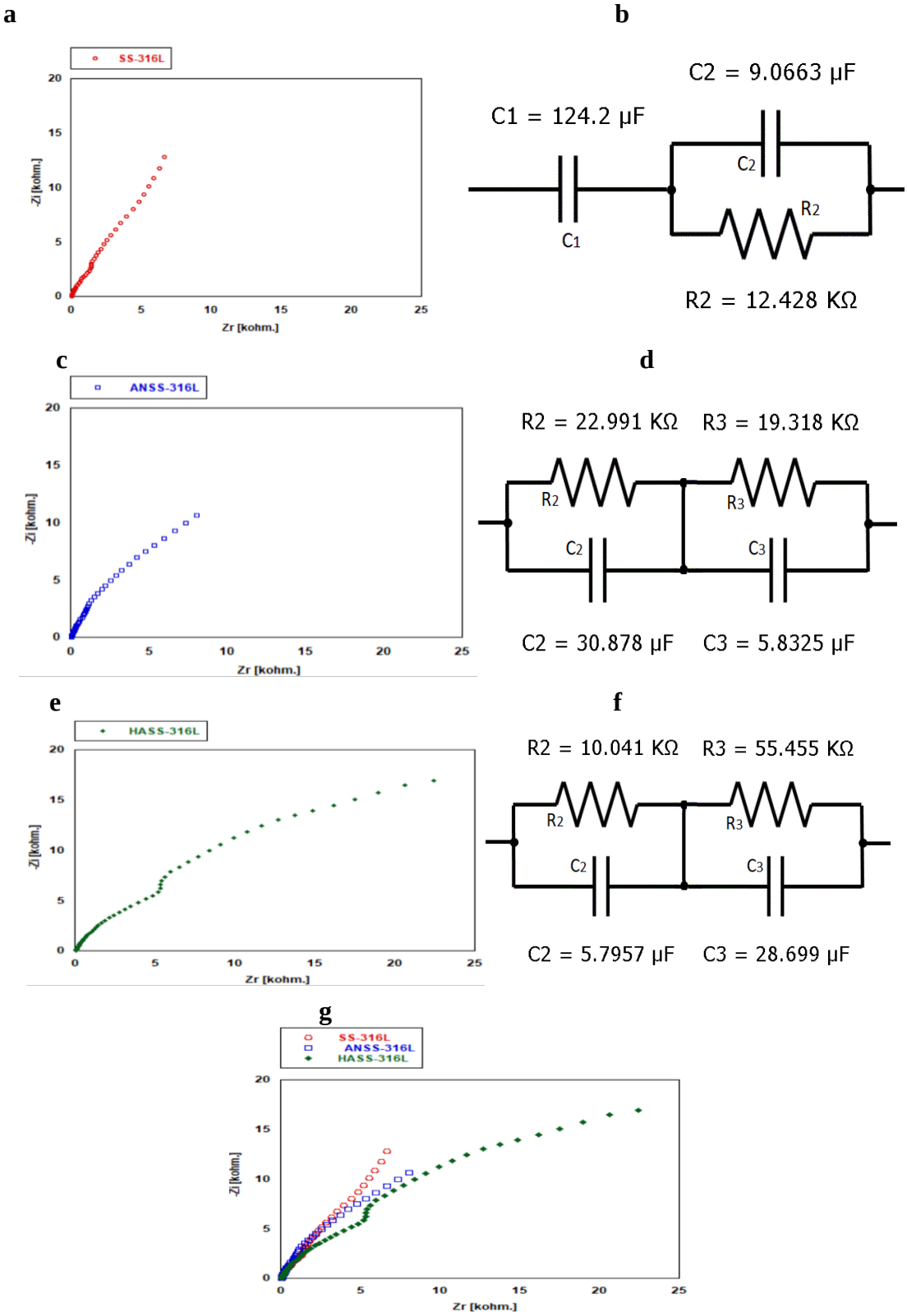

Figure 6. Impedance curve and equivalent circuit of the stainless steel 316L with (c,d,e,f) and without treatment (a,b)

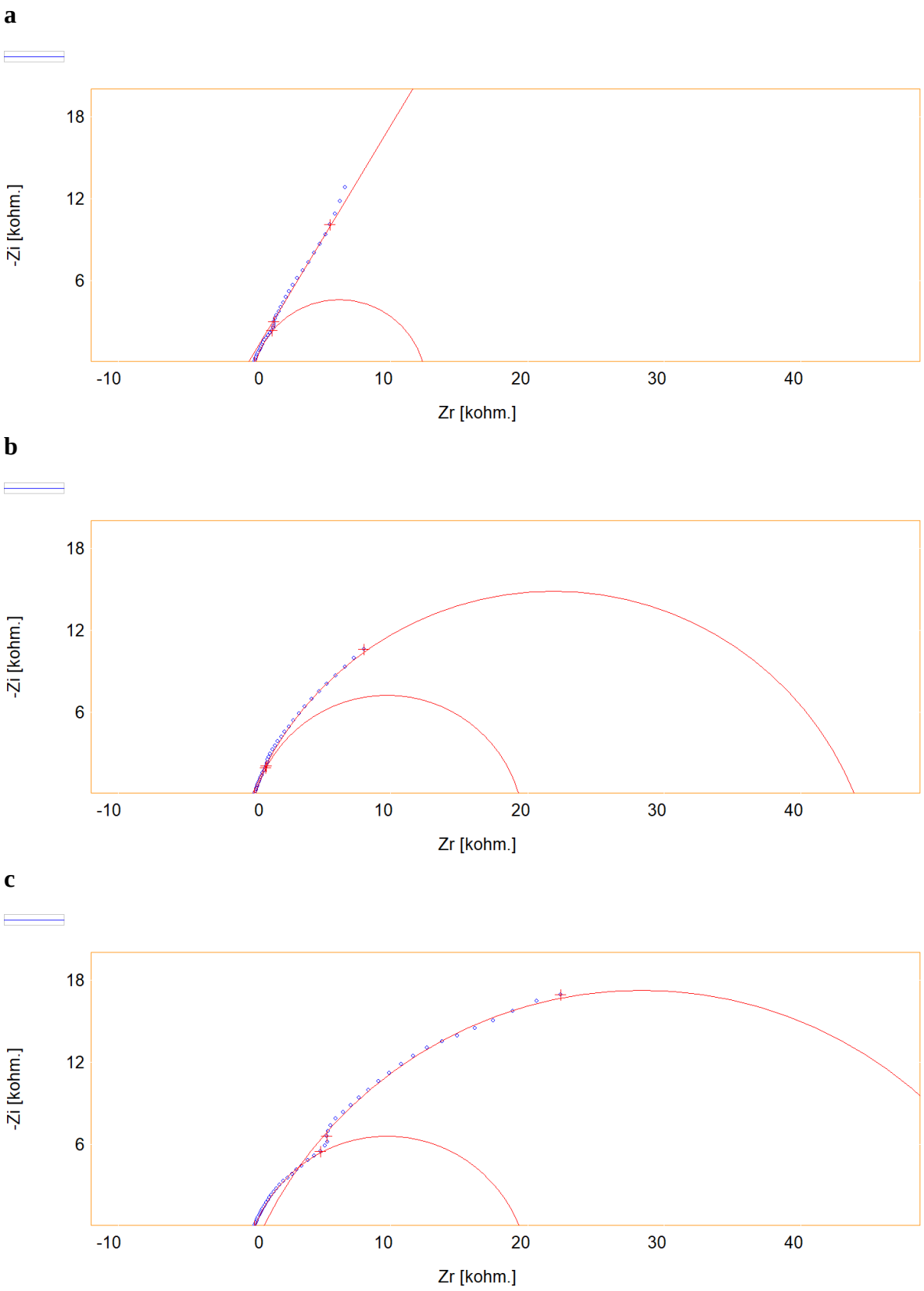

Figure 7. Nyquist diagrams of experimental (circles) and simulated (lines) impedance spectra for three surfaces: (a) untreated (SS-316L), (b) anodized (AN-316L) and (c) deposited (HA-316L)

4. CONCLUSION

An investigation of the corrosion behavior of stainless steel used in orthopedic implants has been conducted using three kinds of samples. In the electrochemical process, hydroxyapatite is formed, as indicated by FTIR and XRD on the stainless-steel substrate, the SEM showed the development of the HAP layer after pre-treating with anodized surface. It was found that the HAP-containing surface had a larger potential, also it had a high polarization resistance than the other HAP-free surfaces, this is confirmed by electrochemical polarization (Tafel) findings obtained from the three surfaces. moreover, the medium used on this investigation is a saline solution functioning as a physiological fluid. As well, electrochemical impedance spectroscopy (EIS) showed that the coated stainless-steel surface was highly resistant to corrosion. we can conclude that the HAP coating serves to improve electrochemical properties and protect metal implants against corrosion.

Declarations of competing interest

The authors declare that they have no known competing financial interests or personal relationships that could have appeared to influence the work reported in this paper.

REFERENCES

[1] N. Eliaz, T. M. Sridhar, U.K. Mudali, and B. Raj, Surf. Eng. 21 (2005) 238.
[2] H. Karahan, and Y. Yücel, Electrochem. Acta 150 (2014) 46.
[3] A.U. Daniels, M.K. Chang, K.P. Andriano, and J. Heller, J. Applied Biomaterials 1 (1990) 57.
[4] M.A. Barbosa, "Corrosion of metallic implants," Handbook of Biomaterial Properties, Second Ed. (2016) pp. 509–548.
[5] Z. Buyong, J. Mech. Behav. Biomed. Mater. 57 (2015) 95.
[6] A. Okada, Y. Uno, J.A. McGeough, K. Fujiwara, K. Doi, K. Uemura, and S. Sano, CIRP Annals 57 (2008) 223.
[7] N.S. Al-Mamun, K. Mairaj Deen, W. Haider, E. Asselin, and I. Shabib, Addit. Manuf. 34 (2020) 101237.
[8] T.P. Chou, C. Chandrasekaran, S. Limmer, C. Nguyen, and G. Z. Cao, J. Mater. Sci. Lett. 21 (2002) 251.
[9] M. Wei, A.J. Ruys, B.K. Milthorpe, C.C. Sorrell, and J.H. Evans, J. Sol-Gel Sci. Technol. 21 (2001) 39.
[10] Y. Parcharoen, P. Kajitvichyanukul, S. Sirivisoot, and P. Termsuksawad, Appl. Surf. Sci. 311 (2014) 54.
[11] M. Stevanović, M. Đošić, A. Janković, V. Kojić, M. Vukašinović-Sekulić, J. Stojanović, J. Odović, M.C. Sakač, K.Y. Rhee, and V. Mišković-Stanković, ACS Biomater. Sci. Eng.

4 (2018) 3994.
[12] D. Arcos, and M. Vallet-Regí, J. Mater. Chem. B 8 (2020) 1781.
[13] A. Fadli, F. Kristin, P. Arini, and S.R. Yenti, J. Phys.: Conference Series 2049 (2021) 012047.
[14] I. Herath, J. Davies, G. Will, P.A. Tran, A. Velic, M. Sarvghad, M. Islam, P.K. Paritala, A. Jaggessar, M. Schuetz, K. Chatterjee, P.K.D.V. Yarlagadda, Electrochim. Acta 416 (2022) 140274.
[15] Y. Zhang, and J. Tao, Trans. Nonferrous Met. Soc. China 16 (2006) 633.
[16] C.C. Yang, C.C. Lin, J.W. Liao, and S.K. Yen, Mater. Sci. Eng. C 33 (2013) 2203.
[17] S. Kannan, A. Balamurugan, and S. Rajeswari, Electrochim. Acta 50 (2005) 2065.
[18] R. Uribe, A. Uvill, L. Fern, O. Bonilla, and G. Gonz, Coating 12 (2022) 440.
[19] S. Y. Jung, H. Hwang, H.S. Jo, S. Choi, H.J. Kim, S.E. Kim, and K. Park, Tannylated Int. J. Mol. Sci. 22 (2021) 4614.